



Zeolitic imidazolate frameworks-67 (ZIF-67) supported PdCu nanoparticles for enhanced catalytic activity in Sonogashira-Hagihara and nitro group reduction under mild conditions

Mohammad Gholinejad^{a, b, *}, Zhwan Naghshbandi^b, Jose M. Sansano^c

^a Department of Chemistry, Mohammad Gholinejad, Zhwan Naghshbandi, Institute for Advanced Studies in Basic Sciences (IASBS), P. O. Box 45195-1159, Gavazang, Zanjan 45137-66731, Iran

^b Mohammad Gholinejad, Research Center for Basic Sciences & Modern Technologies (RBST), Institute for Advanced Studies in Basic Sciences (IASBS), Zanjan 45137-66731, Iran

^c José M. Sansano Departamento de Química Orgánica, Instituto de Síntesis Orgánica and Centro de Innovación en Química Avanzada (ORFEO-CINQA), Universidad de Alicante, Apdo. 99, Alicante E-03080, Spain

ARTICLE INFO

Keywords:

ZIF-67
Palladium
Cobalt
Copper
Sonogashira
Reduction reaction

ABSTRACT

A bimetallic PdCu supported on amine functionalized ZIF-67 is shown to be efficient catalyst in Sonogashira-Hagihara coupling reaction of aryl iodides at room temperature and aryl bromides at 40 °C. In addition, the catalyst is used in the reduction of 4-nitrophenol (4-NP) at room temperature. The analyses of several experiments are developed in order to demonstrate the existence of synergetic affects between Pd, Cu and Co particles in the named reactions. The stability and reusability of this catalyst are also assessed and its efficiency is compared with other reported catalysts in the same transformations.

1. Introduction

The carbon-carbon bond formation is a very important reaction in the organic synthesis, pharmaceutical and agrochemical industries. Among different C-C bond forming reactions, Sonogashira-Hagihara reaction, which involves the coupling of vinyl or aryl halides or triflates with terminal alkyne, is an efficient strategy for the preparation of aryl alkynes and conjugated enynes [1–4]. Generally, this reaction proceeds using palladium catalyst in the presence or absence of a copper co-catalyst. Considering different copper-free Sonogashira-Hagihara reactions and the associated problem of alkyne homocoupling reaction via Glaser coupling, it has been demonstrated that the presence of copper particles, under oxygen-free reaction conditions, increases the efficiency of the reaction [5–9].

In the other side, nitrophenol (NP) derivatives are considered as hazardous pollutants, released from pharmaceutical, plasticizer, paper production, preservative, explosives, and dye industries [10]. The U.S. Environmental Protection Agency (EPA) introduced 4-nitrophenol as non-biodegradable pollutant [11]. The reduction of 4-NP to 4-aminophenol (4-AP) is a very advisable practice to reduce this environ-

mental conflict. Moreover, the resulting 4-AP are employed as a precursor of antipyretic and analgesic drugs, photography, dyes and paints industries [12,13]. Recently, several catalyst containing Cu, Pd and Co are reported for this purpose [14–19].

Recently, a great attention has been paid to the design of multi-metallic catalysts with high performance, as for example, PdCu species in the Sonogashira-Hagihara coupling reaction [20–39] and nitroarene reduction reactions [40–42]. This interest is mainly caused by the known synergistic effect between metals that affect the catalytic behavior of the resulting multi-metallic nanoparticles. Their unique specific chemical and physical properties, compared to monometallic systems, open new advantages and unexpected efficiencies and chemoselectivities in numerous transformations [43–45].

During the last decade, Metal Organic Frameworks (MOFs) have been attracted the attention of researchers due to their inherent physical and chemical properties such as specific surface areas, higher porosity, tunable cavities, special thermal and chemical stability. Zeolite Imidazolate Frameworks (ZIFs) are a new class of MOFs where the transition-metal cation (M) is coordinated by a bridging imidazole ligand with the angle of M-Im-M is 145° [46–49]. As a kind of ZIFs, ZIF-67,

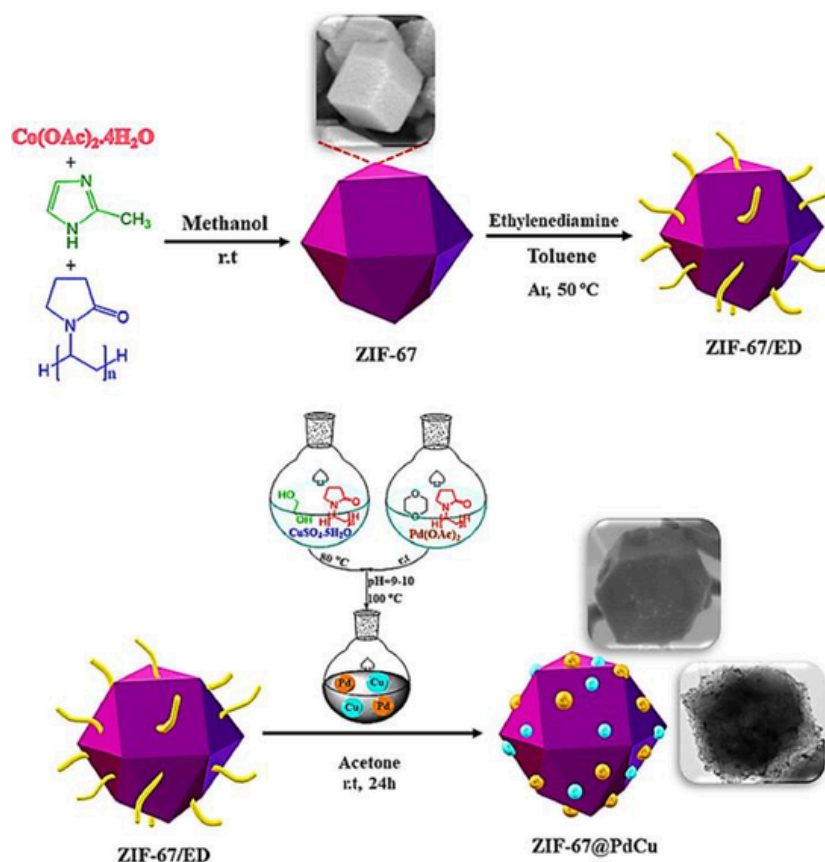
* Corresponding author at: Department of Chemistry, Mohammad Gholinejad, Zhwan Naghshbandi, Institute for Advanced Studies in Basic Sciences (IASBS), P. O. Box 45195-1159, Gavazang, Zanjan 45137-66731, Iran.

E-mail address: gholinejad@iasbs.ac.ir (M. Gholinejad).

<https://doi.org/10.1016/j.mcat.2021.112093>

Received 23 October 2021; Accepted 23 December 2021

2468-8231/© 2021



Scheme 1. Schematic diagram for the preparation of ZIF-67/ED@PdCu.

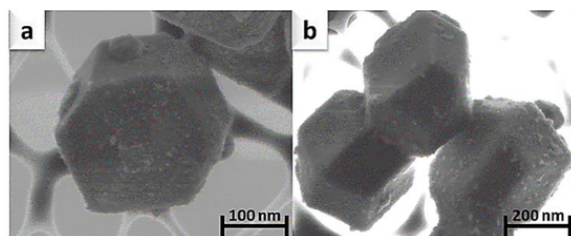


Figure 1. SEM images of ZIF-67@PdCu.

composed of Co^{2+} metal centers and 2-methylimidazolate ligand, the structure of ZIF-67 exhibited a cubic crystal symmetry. ZIFs have been widely applied for gas storage, separation, sensors, drug delivery and catalysis [50–53]. Furthermore, ZIFs were used as heterogeneous catalyst in different organic reactions as well as cross coupling reactions. For example, Zhou's group synthesized Pd@ZIF-67 as catalysts for Heck reactions [54]. Wang's group prepared PdxCu_{1-x}@ZIF-8 bimetallic catalysts studying its applications in the Sonogashira-Hagihara reactions [55]. Mao et al. performed the Suzuki coupling reactions using PdNPs/ZIF-8 [56].

However, to the best of our knowledge there is no precedents in the use of a trimetallic catalyst comprising Pd, Cu and Co neither in Sonogashira nor nitroarene reduction reactions. In this study, we construct a ZIF-67 with cubic morphology and next functionalized with ethylene diamine (ZIF-67/ED) which will serve as support for PdCu nanoparticles (ZIF-67@PdCu).

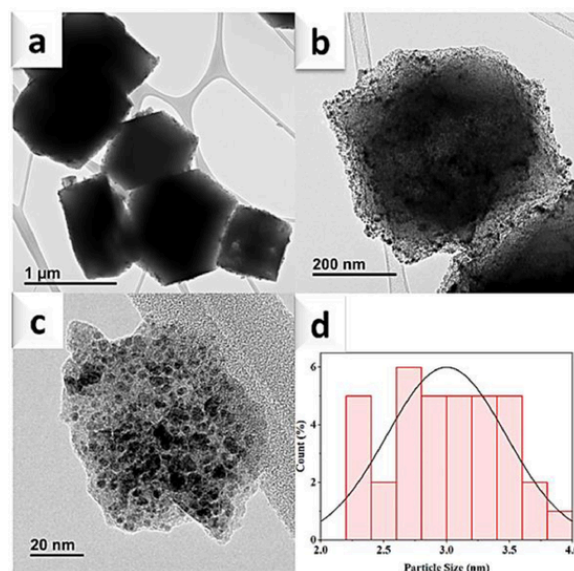


Fig. 2. TEM images and histogram of particle size distribution for ZIF-67@PdCu.

2. Experimental

2.1. Materials and methods

Cobalt acetate tetrahydrate ($\text{Co}(\text{OAc})_2 \cdot 4\text{H}_2\text{O}$), polyvinylpyrrolidone (PVP, MW~10,000), 2-methylimidazole, methanol, ethylenediamine (ED), toluene, copper sulfate pentahydrate $\text{CuSO}_4 \cdot 5\text{H}_2\text{O}$, ethylene glycol, palladium acetate $\text{Pd}(\text{OAc})_2$, dioxane, sodium hydroxide

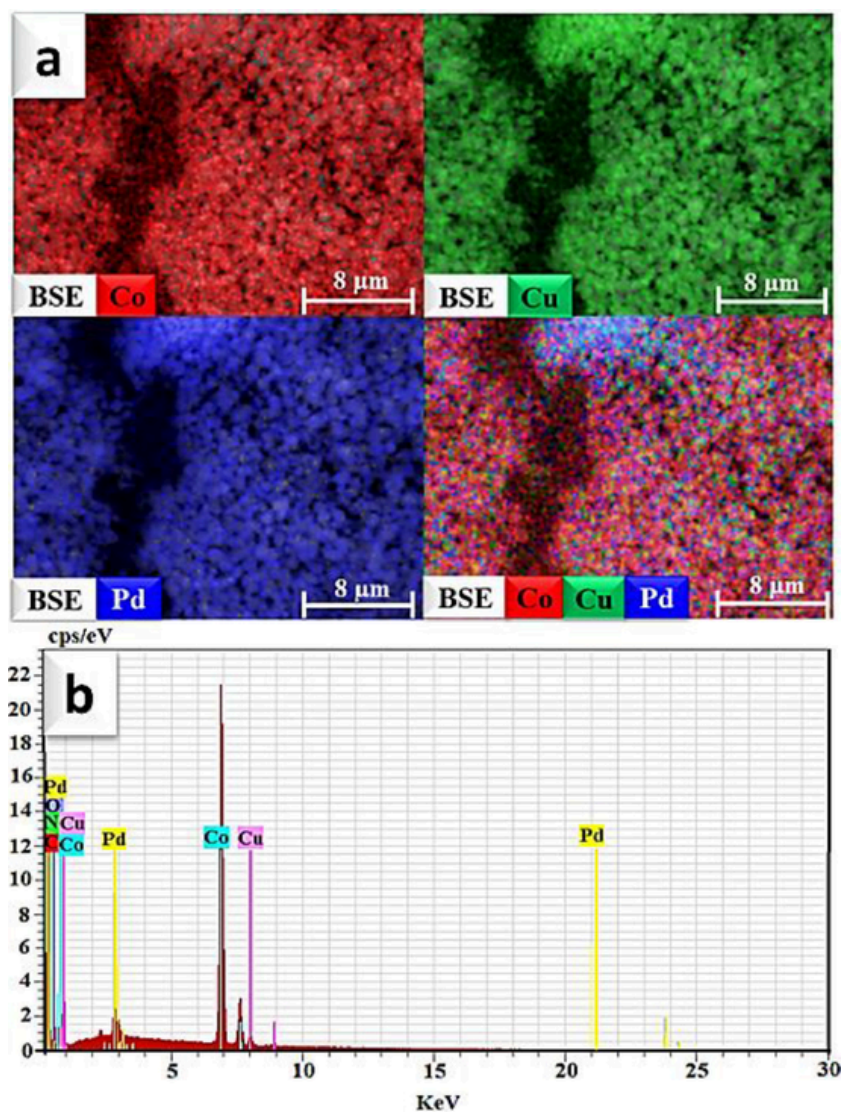


Fig. 3. (a) Elemental mapping and (b) EDX-SEM of ZIF-67@PdCu.

(NaOH), acetone, aryl halides, aryl acetylenes, *N,N*-dimethylacetamide (DMA), 1,4-diazabicyclo[2.2.2]octane (DABCO) were provided from Acros and Merck Millipore Sigma. Reactions were monitored by thin layer chromatography (TLC) using Merck silica gel 60F254 glass plate with 0.25 mm thickness and Varian CP-3800 gas chromatograph. Fourier transform infrared (FT-IR) spectra (KBr disks) were registered on a Bruker optics TENSOR 27 spectrometer. The morphology and structure of the prepared samples were measured by a field-emission scanning electron microscopy (FE-SEM JEOL JSM 840) and transmission electron microscopy (TEM EOL JEM-2010). The SEM mapping was investigated by Hitachi S3000 N. The crystallographic structures of the products were evaluated by X-ray diffractometer (XRD) with Cu K α radiation in the 2θ range from 10° to 80° . Thermogravimetric (TG) analysis was carried out on a thermogravimetric analyzer NETZSCH STA 409 PC/PG with the heating rate of 5 C min^{-1} in the air atmosphere. X-ray photoelectron spectroscopy (XPS) measurements were recorded using a K α spectrometer.

2.2. Method of synthesis of ZIF-67

For the synthesis of ZIF-67, $\text{Co}(\text{OAc})_2 \cdot 6\text{H}_2\text{O}$ (2.4 mmol, 520 mg) and PVP (600 mg) were dissolved in methanol (40 mL), then 2-methylimidazole (0.032 mmol, 2.63 mg) was dispersed in methanol

(40 mL), and both solutions were blended together. The mixture was stirred at room temperature for 24 h and a purple precipitate was obtained. Then, solution was centrifuged, washed several times with methanol and dried at $60\text{ }^\circ\text{C}$.

2.3. Preparation of ZIF-67/ethylenediamine (ED)

For the functionalization of ZIF-67 with ethylene diamine, 300 mg ZIF-67 were dispersed in dry toluene and 1 mL ethylene diamine (30%) was added. The resulting mixture was stirred at $50\text{ }^\circ\text{C}$ for 24 h. Then, the precipitate was separated with centrifugation, washed several times with ethanol and dried at $80\text{ }^\circ\text{C}$ for 1 day.

2.4. Synthesis of ZIF-67@PdCu

$\text{CuSO}_4 \cdot 5\text{H}_2\text{O}$ (0.07 mmol, 18 mg) was dissolved in ethylene glycol (5 mL) and 200 mg PVP was added. The solution was stirred at $80\text{ }^\circ\text{C}$ for 2 h under an argon atmosphere. In another flask, $\text{Pd}(\text{OAc})_2$ (0.16 mmol, 32 mg) and PVP (400 mg) were dissolved in 1,4-dioxane (5 mL) and the mixture was stirred at room temperature for 2 h under an argon atmosphere. Next, the mixing the both solutions, the pH of the solution was adjusted to pH~10 with addition of NaOH (1 M) and the resulting mixture was stirred at $100\text{ }^\circ\text{C}$ for 2 h. Afterwards, the

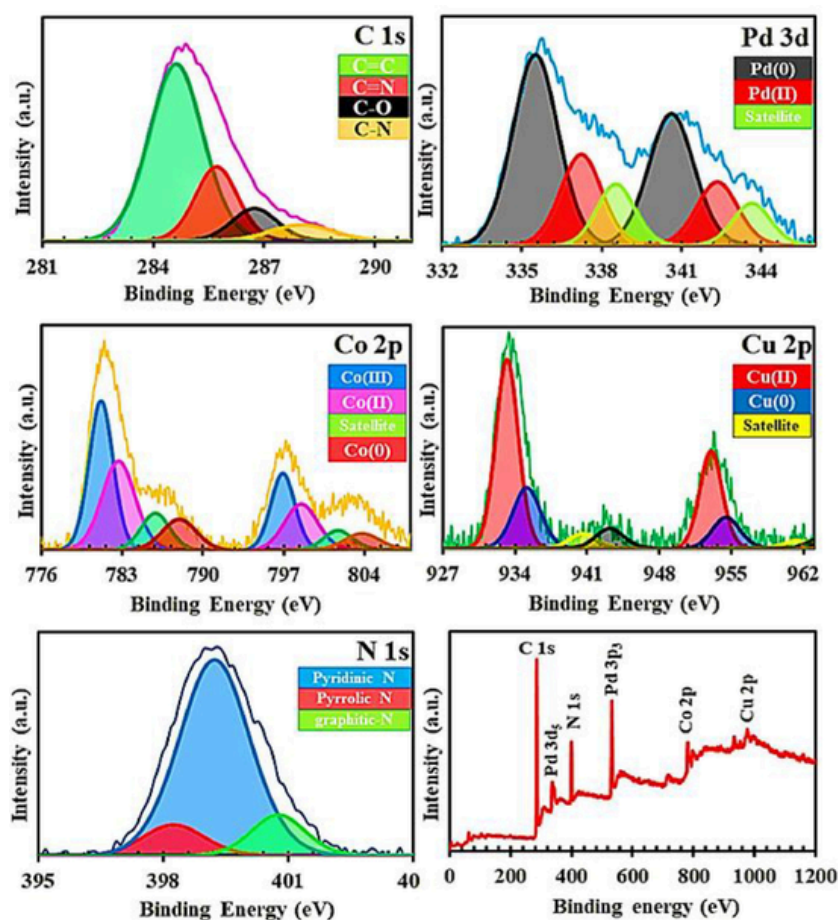


Fig. 4. XPS spectra of ZIF-67@PdCu.

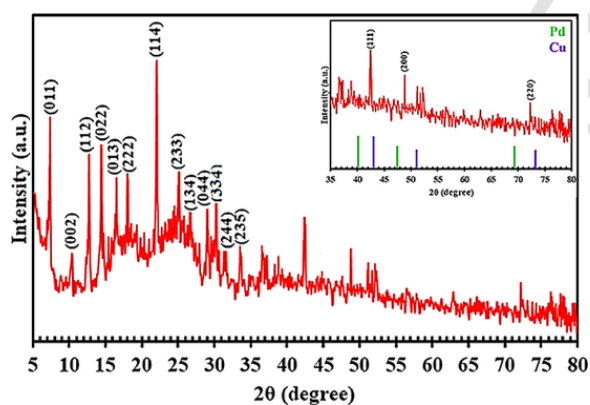


Fig. 5. XRD pattern of ZIF-67@PdCu.

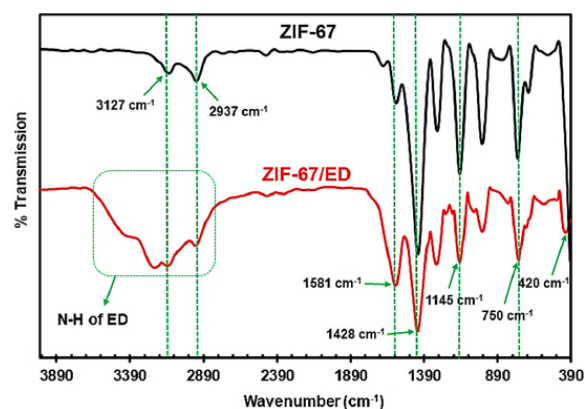


Fig. 6. FT-IR spectra of ZIF-67 and ZIF-67/ED.

obtained solution was cooled to room temperature and concentrated to 5 mL. The resulting suspension was diluted with acetone (5 mL) and the mixture was added to the solution of ZIF-67/ED (300 mg ZIF-67/ED dissolved in 10 mL acetone). The final mixture was stirred at room temperature for 24 h and then centrifuged. The resulting precipitate was washed with dichloromethane and dried at 60 °C affording ZIF-67@PdCu.

2.5. General procedure for Sonogashira reaction

In a 5 mL flask, ZIF-67@PdCu (25 mg) ArX (0.5 mmol) and DABCO (0.75 mmol) were well dispersed in 2 mL of DMA under argon atmosphere. The aryl acetylene (0.75 mmol) was added to the resulting mix-

ture and stirred at 30 °C for ArI and 40 °C for ArBr for 24 h. The progress of the reaction was monitored by TLC and GC. After completion of the reaction, the mixture was extracted with ethyl acetate (3 × 5 mL) and water (10 mL). The residue was purified by column and plate chromatography with hexane and ethyl acetate as eluents. All products were identified by ¹HNMR and ¹³CNMR spectroscopy.

2.6. Catalytic reduction of 4-nitrophenol

To a flask containing 2.5 mL 4-NP solution in neat water (0.12 mM) and 0.2 mL of freshly prepared NaBH₄ in water (0.5 M), 1 mg of the catalyst was added and mixture was stirred at room temperature. The con-

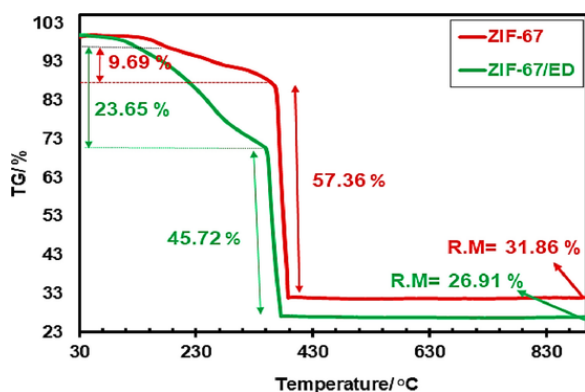


Fig. 1 TGA curves of ZIF-67 and ZIF-67/ED.

version of 4-nitrophenol to 4-aminophenol monitored by UV-Vis spectroscopy by measured absorption spectra.

3. Results and discussion

3.1. Catalyst preparation and characterization

The synthetic routes to the ZIF-67/ED and corresponding PdCu supported on ZIF-67/ED@PdCu are shown in Scheme 1. Briefly, ZIF-67 crystals were prepared using a simple reaction of cobalt acetate and 2-methylimidazole in methanol solvent at room temperature. Afterwards, ZIF-67 was functionalized with ethylenediamine in toluene and the resulting material was treated with prepared PdCu nanoparticles.

The shape and surface of microstructures of ZIF-67@PdCu was studied using field-emission scanning electron microscopy (SEM) and transmission electron microscopy (TEM). The uniform rhombic dodecahedral morphology of ZIF-67@PdCu was confirmed by SEM (Fig. 1) and TEM images (Fig. 2). As it can be observed in TEM images, PdCu NPs

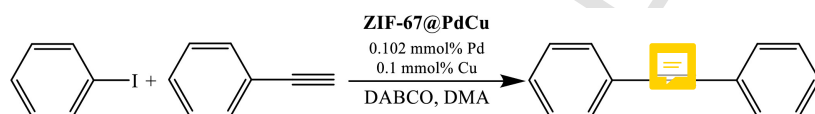
were uniformly dispersed on ZIF 67 surface. More importantly, the crystal structure of ZIF-67 was not changed neither by the functionalization by ED nor by PdCu deposition. The particle size of ZIF-67@PdCu (approximately 100 particles) was estimated 3 ± 0.25 nm, according to the particle size histogram in Fig. 2d. The elemental mapping (Fig. 3a) demonstrated a uniform and homogeneous distribution of Pd, Cu and Co particles on the ZIF-67@PdCu. The energy-dispersive X-ray (EDX) spectra (Fig. 3b) of the representative sample reported that composition of ZIF-67@PdCu consisted of 54.7 wt% C, 16.96 wt% N, 7.41 wt% O, 18.75 wt% Co, 0.99 wt% Cu and 1.45 wt% Pd. The loading of Pd and Cu on ZIF-67@PdCu investigated using ICP analysis was 1.27 mg/L for Cu and 2.17 mg/L for Pd.

Additionally, the X-ray photoelectron spectroscopy (XPS) (Fig. 4) confirmed the presence of Co, Pd, Cu, C and N on the surface of ZIF-67@PdCu. The high-resolution C 1s spectra shown peaks at 284.7, 285.8, 286.9 and 288.2 eV corresponding to C=C, C=N, C—O and C—N, respectively. The binding energy N 1s centered at 398.4, 399.3 and 400.8 eV represented pyridinic, pyrrolic and graphitic N, respectively. The Co 2p spectra revealed four peaks corresponding to Co^{3+} , Co^{2+} , Co^0 and satellite peaks. The peaks at 781.3 and 797.2 eV correlated with Co^{3+} 2p_{3/2} and 2p_{1/2}, as well as Co^{2+} 2p_{3/2} and 2p_{1/2} peaks located at 783.0 and 798.8 eV, respectively [57,58]. The peaks at 788.0 and 803.9 eV were attributed to metallic Co (Co^0) [59]. The Pd XPS spectra exhibited two prominent peaks at 335.6 and 340.7 eV assigned to Pd(0) 3d_{5/2} and 3d_{3/2}, respectively. The peaks at 337.3, 342.4 eV were ascribed to Pd(II) 3d_{5/2} and 3d_{3/2}. For XPS spectra of Cu 2p, the Cu (II) and Cu(0) peaks appeared at binding energy at 933.4 and 935.3 eV for 2p_{3/2}, also 953.1 and 954.6 eV for 2p_{1/2}, respectively [60,61].

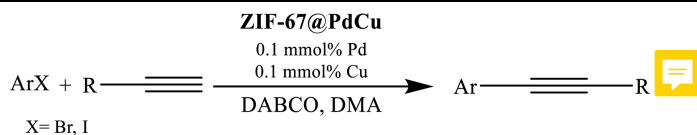
The crystalline structure of ZIF-67@PdCu was studied using the powder X-ray diffraction (XRD) pattern (Fig. 5). The notable peaks at $2\theta = 7.4^\circ, 10.4^\circ, 12.7^\circ, 14.8^\circ, 16.5^\circ, 18.0^\circ, 22.1^\circ, 24.5^\circ, 26.7^\circ, 29.5^\circ, 30.6^\circ, 31.6^\circ$ and 32.5° were assigned to (011), (002), (112), (022), (013), (222), (114), (233), (134), (044), (334), (244) and (235) plans of ZIF-67 [62–64]. The diffraction peaks of crystalline Pd were located at

Table 1

Optimization of the reaction condition for the coupling of iodobenzene and phenyl acetylene catalyzed by ZIF-67@PdCu.



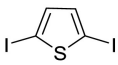
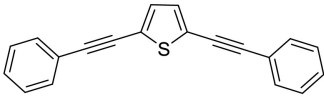
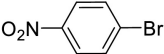
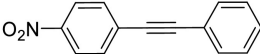
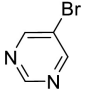
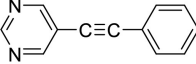
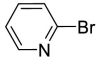
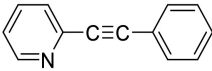
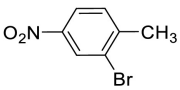
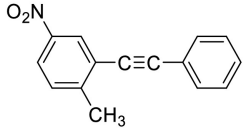
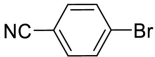
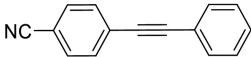
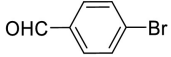
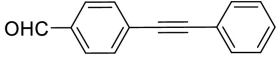
Yield%	Base	Solvent	Entry
1	DABCO	H ₂ O	1
2	K ₂ CO ₃	H ₂ O	2
1	NEt ₃	H ₂ O	3
3	DABCO	Ethanol	4
1	K ₂ CO ₃	Ethanol	5
81	DABCO	DMF	6
2	K ₂ CO ₃	DMF	7
35	NEt ₃	DMF	8
3	<i>t</i> -BuOK	DMF	9
91	DABCO	Toluene	10
15	K ₂ CO ₃	Toluene	11
42	NEt ₃	Toluene	12
1	<i>t</i> -BuOK	Toluene	13
63	DABCO	PEG	14
1	K ₂ CO ₃	PEG	15
22	NEt ₃	PEG	16
2	<i>t</i> -BuOK	PEG	17
98	DABCO	DMA	18
30	NaOH	DMA	19
3	<i>t</i> -BuOK	DMA	20
20	K ₂ CO ₃	DMA	21
50	NEt ₃	DMA	22

Table 2Sonogashira coupling reaction of aryl halides with aryl acetylene in the presence of ZIF-67@PdCu as catalyst. ^[a], ^[b]

Entry	Substrate (Ar)	R	Product	Yield (%)
1		C ₆ H ₅		90
2		C ₆ H ₅		100
3		4-MeC ₆ H ₄		90 ^c
4		C ₆ H ₅		92
5		C ₆ H ₅		80 ^c
6		C ₆ H ₅		98
7		C ₆ H ₅		86 ^c
8		C ₆ H ₅		100
9		C ₆ H ₅		98
10		C ₆ H ₅		82
11		C ₆ H ₅		86
12		HOCH ₂		100
13		HOCH ₂		98
14		4-MeC ₆ H ₄		90 ^c
15		C ₆ H ₅		95
16		CH ₃ (CH ₂) ₅		92

(continued on next page)

Table 2 (continued)

17		C ₆ H ₅		90
18		C ₆ H ₅		85 ^c
19		C ₆ H ₅		85
20		C ₆ H ₅		80
21		C ₆ H ₅		79 ^c
22		C ₆ H ₅		86
23		C ₆ H ₅		92

20 = 40.3°, 46.7° and 68.2°, whilst the diffraction peaks of crystalline Cu were placed at 2θ = 43.3°, 50.4° and 74.1°. It should be noted that between 2θ values for pure Pd and Cu, three new peaks at 2θ = 41.1°, 47.6° and 69.6° corresponded to (111), (200) and (220) of PdCu species confirming the formation of PdCu metal alloy [65,66].

The FT-IR spectra of ZIF-67 was plotted before and after amine grafting (Fig. 6). All of the peak position of FT-IR spectra were identical for ZIF-67 and ZIF-67/ED except the new peak at 3381 cm⁻¹ band related to N-H group observed in the ZIF-67/ED. The FT-IR spectra of ZIF-67 showed peaks at 3127 and 2937 cm⁻¹ corresponding to the aromatic C-H and aliphatic C-H bonds, respectively. The band located at 1581 cm⁻¹ represented the C=C stretch and the peaks at 1145 and 1428 cm⁻¹ were assigned the C-N stretch. The 420 cm⁻¹ peaks introduced the Co-N stretching mode [67–69].

The thermal stability of ZIF-67 and ZIF-67/ED was surveyed by thermogravimetric analysis (TGA) (Fig. 7). In the TGA plot, it was observed a sharp weight-loss around 360 °C for ZIF-67 and 350 °C for ZIF-67/ED, corresponding to the decomposition ZIF-67. Increasing weight loss for ZIF-67/ED between 100 and 350 °C confirm successful attachment of ED.

The catalytic performance of ZIF-67@PdCu was next evaluated in Sonogashira-Hagihara coupling reactions (Table 2). Initially, the ZIF-67@PdCu catalyst was optimized by testing different bases, solvents, catalyst loadings and temperature. The evaluation of parameters was performed in the reaction of iodobenzene and phenylacetylene under inert atmosphere (i.e. argon) and the results presented in Table 1. As can be seen in Table 1, the *N,N*-dimethylacetamide (DMA) was the selected solvent versus different solvents such as H₂O, ethanol, DMF, toluene and PEG. 1,4-Diazabicyclo[2.2.2]octane (DABCO) was the most appropriate base, rather than K₂CO₃, NaOH, *t*-BuOK or NEt₃. Also, using 10 mg of catalyst, containing 0.102 mmol% of Pd and 0.1 mmol% of Cu, at room temperature provided the best yield (98%) (Table 1, entry 18). On the other hand, under the optimized conditions the catalytic activity of ZIF-67@PdCu was further studied in the Sonogashira-Hagihara coupling reactions with other functionalized substrates (Table 2). The

reaction of assorted aryl iodides containing both electron-donating and electron-withdrawing groups with terminal alkynes took place in high to excellent yields (80–100%) (Table 2, entries 1–17). The aryl iodides bearing electron withdrawing groups (-NO₂, CHO, -CN) gave higher yields than aryl iodides having electron donating groups (-CH₃, -OCH₃). We further studied applications of ZIF-67@PdCu for Sonogashira-Hagihara reaction of aryl bromides. Reaction of 1-bromo-4-nitrobenzene with phenylacetylene under optimized reaction condition gave 60% yield. Therefore, Sonogashira reaction of aryl bromides using ZIF-67@PdCu catalyst were studied at 40 °C. Using the optimized conditions desired coupling products from the reaction of aryl bromides with alkynes, were obtained in 79–94% yields (Table 2, entry 18–23). When aryl chlorides were employed, the products were formed in low yields even at 100 °C for 24 h. To exhibit the important effect of the Pd, Cu and ZIF-67 in Sonogashira reaction, the reaction of iodobenzene with phenylacetylene was performed in the presence of ZIF-67, ZIF-67@Pd, ZIF-67@Cu and PdCu individually as catalysts. The results illustrated that the reaction accomplished with ZIF-67 was not produced, a 38% of the final product was obtained using ZIF-67@Pd, a 20% with ZIF-67@Cu and a 56% employing PdCu under optimized reaction conditions.

Next, we further studied catalytic activity of ZIF67@PdCu in the reduction of 4-NP to 4-AP. Generally, in accordance with UV-Vis absorbance (Fig. 8), the absorption peak of 4-NP decreased at a wavelength of 400 nm and the new peak, related to 4-AP, appeared at a wavelength of 300 nm. Also, during the catalytic reduction, the color of the solution changed from yellow (4-NP) to colorless (4-AP). It should be noted that the peak related to 4-NP at 400 nm remained unchanged even after 10 h in the absence of the catalyst [70–72]. Results showed that using ZIF67@PdCu in the presence of NaBH₄ the reduction of 4-NP to 4-AP was immediately completed (1 s) (Fig. 8a). It was also observed that the ZIF-67@PdCu exhibited higher catalytic activity than ZIF-67@Pd (Fig. 8b), ZIF-67@Cu (Fig. 8c) and ZIF-67 (Fig. 8d). The apparent rate constants (k_{app}) obtained for all catalysts were calculated using $\ln(C_t/C_0) = \ln(A_t/A_0) = -k_{app} t$ equation, where C_t and C_0 represented

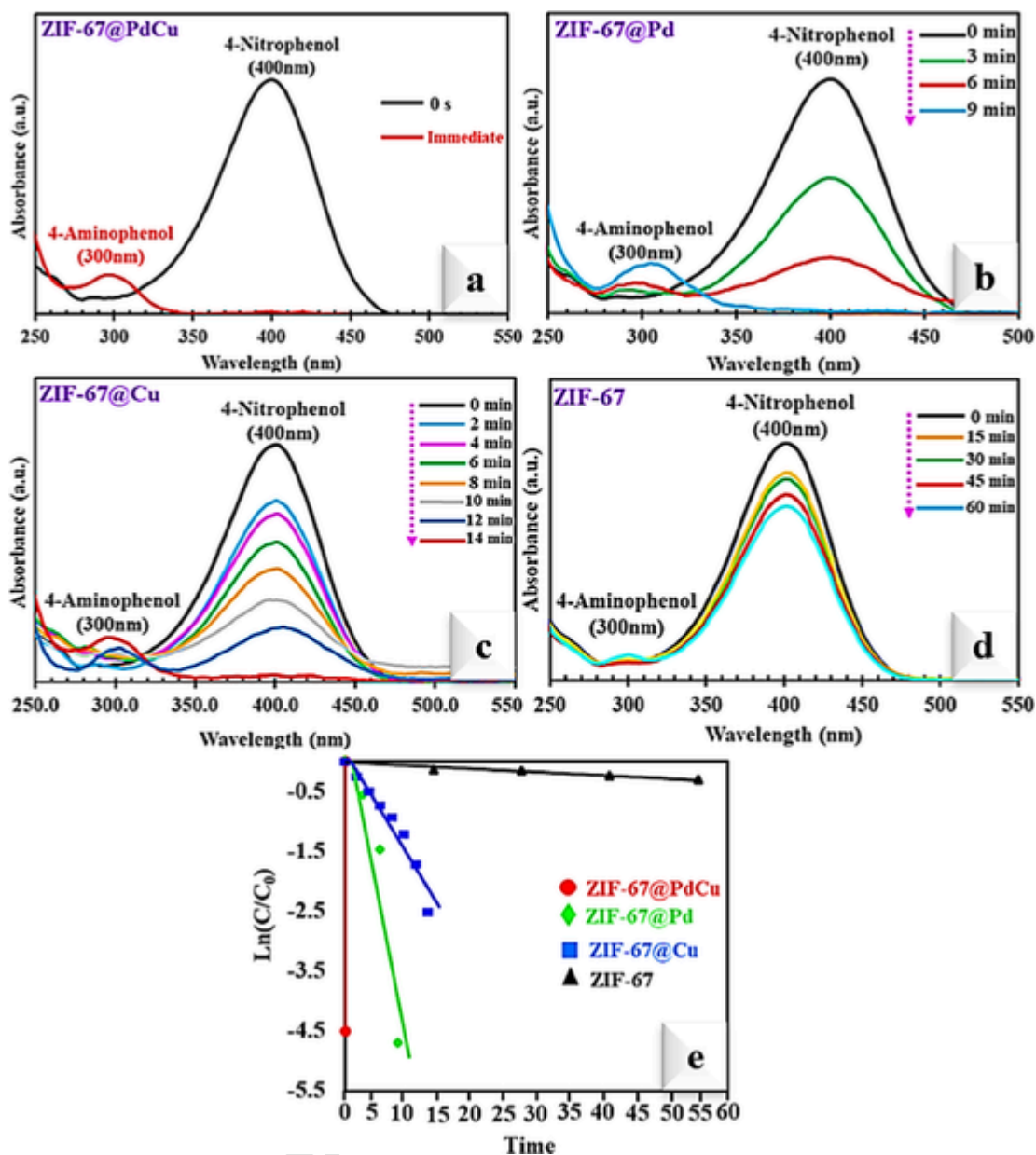


Fig. 8 UV-Vis absorption spectra of 4-NP to 4-AP after reduction with NaBH_4 in the presence of (a) ZIF-67@PdCu (b) ZIF-67@Pd (c) ZIF-67@Cu (d) ZIF-67 (e) Plots of $\ln(C/C_0)$ versus reaction times for the catalytic reduction of 4-NP using different catalysts.

Table 3

Catalytic activity of ZIF-67@PdCu, ZIF-67@Pd, ZIF-67@Cu and ZIF-67 in hydrogenation of 4-NP at ambient temperature.

$K_{\text{nor}}(\text{g}^{-1} \text{s}^{-1})$	$K_{\text{app}}(\text{s}^{-1})$	Conversion%	Time	Catalyst
4610	4.61	99.1	Immediate (1s)	ZIF-67@PdCu
9	9×10^{-3}	99	9 min	ZIF-67@Pd
4	4×10^{-3}	96.52	14 min	ZIF-67@Cu
0.085	8.3×10^{-5}	26.22	60 min	ZIF-67

the concentration of 4-NP at time t and the time of initial concentration, respectively. As well as, A_t and A_0 represented the absorbance of 4-NP at 400 nm at time t and 0 [73]. The k_{app} values of ZIF-67@PdCu, ZIF-67@Pd, ZIF-67@Cu and ZIF-67 were estimated in 4.61 s^{-1} , 0.009 s^{-1} , 0.004 s^{-1} and 0.000083 s^{-1} , respectively (Table 3). The rate constants k_{app} of ZIF-67@PdCu were compared with the other ones reported for other catalysts reported previously (Table 4) [74–82]. In conclusion, it is demonstrated that ZIF-67@PdCu has a superior rate and efficiency.

Table 4

Comparison of the rate constants of other catalysts reported for 4-NP reduction with NaBH_4 .

Reference	$K_{\text{app}} (\text{min}^{-1})$	Catalyst
[74]	0.218	CS-CNTs-PdNPs
[75]	0.0348	CS/GA/RGO/Pd
[76]	0.12	Pd-GA/RGO
[77]	0.288	$\text{Cu}_x\text{O}/\text{C}$
[78]	1.74	$\text{Cu}/\text{Cu}_x\text{O}/\text{C}$
[79]	4.185	$\text{Cu}/\text{Co}/\text{NCF}$
[80]	0.252	CoO_x/CN
[81]	2.6	$\text{Cu}(0.25)/\text{ZIF-Co}/\text{Zn}$
[82]	3.54	N-Co@C-800-3
This work	276.6	ZIF-67@PdCu

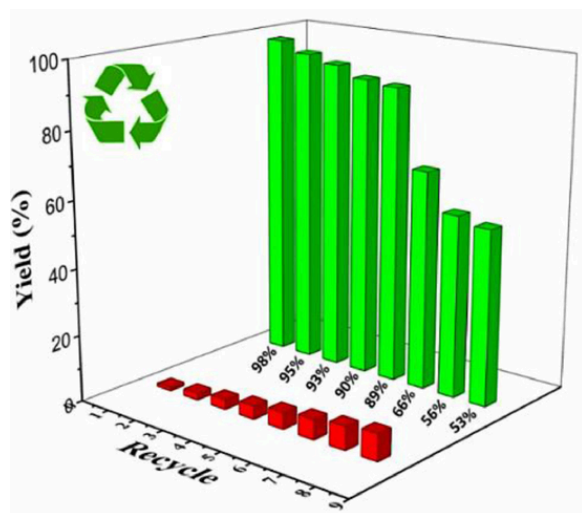


Fig. 9. Reusability of the ZIF-67@PdCu catalyst in the Sonogashira reaction of iodobenzene with phenyl acetylene under optimized conditions.

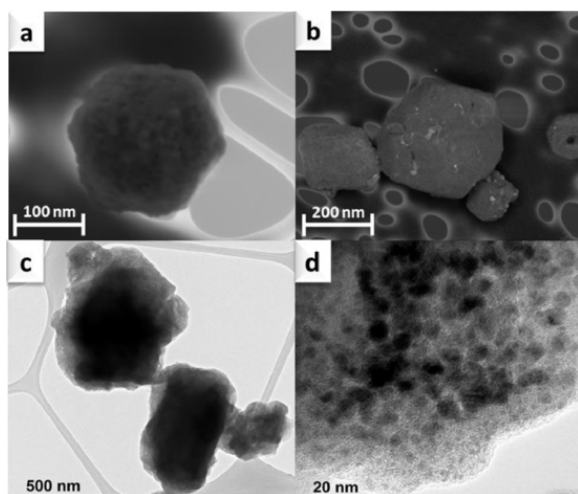


Fig. 10. a, b) SEM and (c, d) images of reused ZIF-67@PdCu catalyst after 5 runs.

The stability and recyclability of catalysts are essential parameters for developing heterogeneous catalysts and industrial usage. In this regard, the reusability of ZIF-67@PdCu catalyst was checked in the reaction of iodobenzene with phenyl acetylene under the optimized reaction conditions. For this purpose, after completing the reaction, the catalyst was collected by centrifugation, washed with water and ethanol and after drying used in another batch of the reaction. According to Fig. 9, the ZIF-67@PdCu catalyst was successfully recycled for 5 consecutive runs giving 89% yield. However, after 6th run the efficiency of the catalyst notably decreased. The reused catalyst after 5th run was characterized using XPS, SEM and TEM analysis. The SEM and TEM images of reused ZIF-67@PdCu catalyst demonstrated more or less similar morphology to fresh one (Fig. 10). XPS spectra of reused ZIF-67@PdCu catalyst in C, N, Co and Cu showed similar pattern to fresh one. However, in the case of Pd, results showed the reduction of all Pd (II) species to Pd (0) (Fig. 11) occurred.

4. Conclusion

In summary, the ZIF-67@PdCu rhombic dodecahedral structure was successfully synthesized of PdCu embedded in ethylenediamine functionalized ZIF-67 by a simple method and characterized by different techniques. The as-prepared ZIF-67@PdCu was applied as an efficient catalyst in the Sonogashira-Hagihara coupling reaction of aryl halides (-I and -Br) with aryl acetylenes in DMA as a solvent using DABCO as a base and 0.102 mmol% Pd at room temperature for aryl iodides and 40 °C for aryl bromides within 24 h. The evaluations for aryl chlorides as a substrate in Sonogashira reactions showed low yields at 100 °C for 24 h. The catalytic performance of ZIF-67@PdCu was higher than to ZIF-67, ZIF-67@Pd, ZIF-67@Cu and PdCu due to the synergistic effect between Pd, Cu and ZIF-67. The ZIF-67@PdCu exhibited an excellent catalytic performance in reduction of 4-NP with the reaction rate constant 4.61 s⁻¹. The best catalytic activity of ZIF-67@PdCu was compared with the less efficient ZIF-67@Pd, ZIF-67@Cu and ZIF-67 for 4-NP catalysts. The introduced catalyst demonstrated superior stability and was recycled up to for 5 runs without any significant lose in catalytic activity. Our work provided a simple way to perform Sonogashira coupling reactions at room temperature using the fabrication of highly efficient and recoverable ZIF-67@PdCu catalyst.

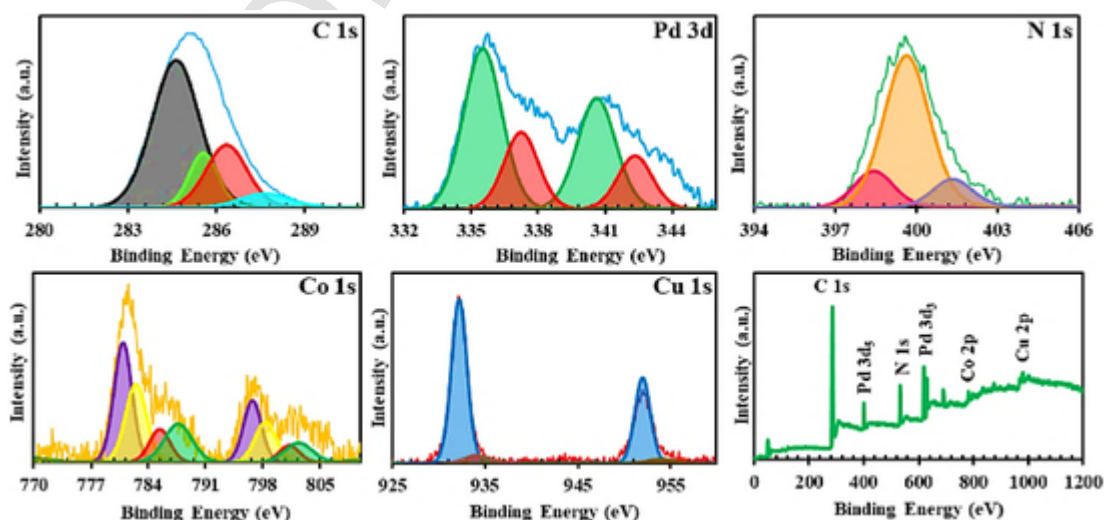


Fig. 11. XPS spectra of reused ZIF-67@PdCu catalyst after 5 runs.

Declaration of Competing Interest

The authors declare that they have no known competing financial interests or personal relationships that could have appeared to influence the work reported in this paper.

Acknowledgements

The authors are grateful to Institute for Advanced Studies in Basic Sciences (IASBS) Research Council and Iran National Science Foundation (INSF-Grant number of 4003055) for support of this work. We are also thankful for financial support to the Spanish Ministerio de Economía y Competitividad (MINECO) (projects CTQ2013-43446-P and CTQ2014-51912-REDC), the Spanish Ministerio de Economía, Industria y Competitividad, Agencia Estatal de Investigación (AEI) and Fondo Europeo de Desarrollo Regional (FEDER, EU) (projects CTQ2016-76782-P, CTQ2016-80375-P, CTQ2017-82935-P and PID2019-107268GB-I00), the Generalitat Valenciana (IDIFEDER/2021/013) and the University of Alicante. Special thanks to Ms. Dehghan Hesami for her technical assistant.

References

- L. Yin, J. Liebscher, Carbon-carbon coupling reactions catalyzed by heterogeneous palladium catalysts, *Chem. Rev.* 107 (2007) 133–173, <https://doi.org/10.1021/cr0505674>.
- P. Taladriz-Blanco, P. Hervés, J. Pérez-Juste, Supported Pd nanoparticles for carbon-carbon coupling reactions, *Top. Catal.* 56 (2013) 1154–1170, <https://doi.org/10.1007/s11244-013-0082-6>.
- M. Gholinejad, Z. Naghsbandi, C. Nájera, Carbon-derived supports for palladium nanoparticles as catalysts for carbon-carbon bonds formation, *ChemCatChem* 11 (2019) 1792–1823, <https://doi.org/10.1002/cctc.201802101>.
- K.C. Nicolaou, P.G. Bulger, D. Sarlah, Palladium-catalyzed cross-coupling reactions in total synthesis, *Angew. Chem. Int. Ed.* 44 (2005) 4442–4489, <https://doi.org/10.1002/anie.200500368>.
- K. Hong, M. Sajjadi, J.M. Suh, K. Zhang, M. Nasrollahzadeh, H.W. Jang, R.S. Varma, M. Shokouhimehr, Palladium nanoparticles on assorted nanostructured supports: applications for suzuki, heck, and sonogashira cross-coupling reactions, *ACS Appl. Nano Mater.* 3 (2020) 2070–2103, <https://doi.org/10.1021/acsnm.9b02017>.
- A. Dewan, M. Sarmah, U. Bora, A.J. Thakur, A green protocol for ligand, copper and base free Sonogashira cross-coupling reaction, *Tetrahedron Lett.* 57 (2016) 3760–3763, <https://doi.org/10.1016/j.tetlet.2016.07.021>.
- P. Rollet, W. Kleist, V. Dufaud, L. Djakovitch, Copper-free heterogeneous catalysts for the Sonogashira cross-coupling reaction: preparation, characterisation, activity and applications for organic synthesis, *J. Mol. Catal. A Chem.* 241 (2005) 39–51, <https://doi.org/10.1016/j.molcata.2005.05.046>.
- L. Djakovitch, P. Rollet, Sonogashira cross-coupling reactions catalysed by copper-free palladium zeolites, *Adv. Synth. Catal.* 346 (2004) 1782–1792, <https://doi.org/10.1002/adsc.200404141>.
- M. Karak, L.C.A. Barbosa, G.C. Hargaden, Recent mechanistic developments and next generation catalysts for the Sonogashira coupling reaction, *RSC Adv.* 4 (2014) 53442–53466, <https://doi.org/10.1039/c4ra09105a>.
- J. Xia, G. He, L. Zhang, X. Sun, X. Wang, Hydrogenation of nitrophenols catalyzed by carbon black-supported nickel nanoparticles under mild conditions, *Appl. Catal. B Environ.* 180 (2016) 408–415, <https://doi.org/10.1016/j.apcatb.2015.06.043>.
- H. Materials, Quality Criteria For Water, US Environmental Protection Agency, 1976.
- M. Ma, Y. Yang, W. Li, R. Feng, Z. Li, P. Lyu, Y. Ma, Gold nanoparticles supported by amino groups on the surface of magnetite microspheres for the catalytic reduction of 4-nitrophenol, *J. Mater. Sci.* 54 (2019) 323–334, <https://doi.org/10.1007/s10853-018-2868-1>.
- Y. Guo, L. Zhang, X. Liu, B. Li, D. Tang, W. Liu, W. Qin, Synthesis of magnetic core-shell carbon dot@MFe₂O₄ (M = Mn, Zn and Cu) hybrid materials and their catalytic properties, *J. Mater. Chem. A* 4 (2016) 4044–4055, <https://doi.org/10.1039/c5ta10708c>.
- A.A. Kassem, H.N. Abdelhamid, D.M. Fouad, S.A. Ibrahim, Catalytic reduction of 4-nitrophenol using copper terephthalate frameworks and CuO@C composite, *J. Environ. Chem. Eng.* 9 (2021) 104401, <https://doi.org/10.1016/j.jece.2020.104401>.
- W. Zhao, S. Yang, C. Guo, J. Yang, Y. Liu, One-step fabrication of Fe₃O₄-Cu nanocomposites: high-efficiency and low-cost catalysts for reduction of 4-nitrophenol, *Mater. Chem. Phys.* 260 (2021) 124144, <https://doi.org/10.1016/j.matchemphys.2020.124144>.
- T. Liu, Y. Sun, B. Jiang, W. Guo, W. Qin, Y. Xie, B. Zhao, L. Zhao, Z. Liang, L. Jiang, Pd nanoparticle-decorated 3D-printed hierarchically porous TiO₂ scaffolds for the efficient reduction of a highly concentrated 4-nitrophenol solution, *ACS Appl. Mater. Interfaces* 12 (2020) 28100–28109, <https://doi.org/10.1021/acsami.0c03959>.
- C. Wang, Y. Chen, S. Feng, N. Zhang, L. Shen, K. Zhang, B. Yang, The preparation of hollow Fe₃O₄/Pd@C NCs to stabilize subminiature Pd nanoparticles for the reduction of 4-nitrophenol, *New J. Chem.* 44 (2020) 4869–4876.
- X.B. Xie, C. Ni, H. Yu, W. Du, X. Sun, D. Sun, Facile fabrication of Co@C nanoparticles with different carbon-shell thicknesses: high-performance microwave absorber and efficient catalyst for the reduction of 4-nitrophenol, *CrystEngComm* 22 (2020) 4591–4601, <https://doi.org/10.1039/d0ce00250j>.
- H. Shin, S. Oh, H. Jun, M. Oh, Porous composites embedded with Cu and Co nanoparticles for efficient catalytic reduction of 4-nitrophenol, *Bull. Korean Chem. Soc.* 42 (2021) 303–308, <https://doi.org/10.1002/bkcs.12141>.
- P. Veerakumar, P. Thanasekaran, K.L. Lu, S. Bin Liu, S. Rajagopal, Functionalized silica matrices and palladium: a versatile heterogeneous catalyst for suzuki, heck, and sonogashira reactions, *ACS Sustain. Chem. Eng.* 5 (2017) 6357–6376, <https://doi.org/10.1021/acssuschemeng.7b00921>.
- S. Diyarbakir, H. Can, Ö. Metin, Reduced graphene oxide-supported cupd alloy nanoparticles as efficient catalysts for the sonogashira cross-coupling reactions, *ACS Appl. Mater. Interfaces* 7 (2015) 3199–3206, <https://doi.org/10.1021/am507764u>.
- S.J. Hoseini, N. Aramesh, M. Bahrami, Effect of addition of iron on morphology and catalytic activity of PdCu nanoalloy thin film as catalyst in Sonogashira coupling reaction, *Appl. Organomet. Chem.* 31 (2017) 1–9, <https://doi.org/10.1002/aoc.3675>.
- D.N. Oleksyzszen, B.L. Albuquerque, D.D.O. Silva, G.L. Tripodi, D.C. De Oliveira, J.B. Domingos, Core-shell PdCu bimetallic colloidal nanoparticles in Sonogashira cross-coupling reaction: mechanistic insights into the catalyst mode of action, *Nanoscale* 12 (2020) 1171–1179, <https://doi.org/10.1039/c9nr09075d>.
- M. Gholinejad, J. Ahmadi, C. Nájera, M. Seyedhamzeh, F. Zareh, M. Kompany-Zareh, Graphene quantum dot modified Fe₃O₄ nanoparticles stabilize PdCu nanoparticles for enhanced catalytic activity in the sonogashira reaction, *ChemCatChem* 9 (2017) 1442–1449, <https://doi.org/10.1002/cctc.201601519>.
- W. Xu, H. Sun, B. Yu, G. Zhang, W. Zhang, Z. Gao, Sonogashira couplings on the surface of montmorillonite-supported Pd/Cu Nanoalloys, *ACS Appl. Mater. Interfaces* 6 (2014) 20261–20268, <https://doi.org/10.1021/am505798y>.
- Z. Wei, Z. Xie, L. Gao, Y. Wang, H. Sun, Y. Jian, G. Zhang, L. Xu, J. Yang, W. Zhang, Z. Gao, Highly crystallized Pd/Cu nanoparticles on activated carbon: an efficient heterogeneous catalyst for sonogashira cross-coupling reaction, *Catalysts* 10 (2020) 1–11, <https://doi.org/10.3390/catal10020192>.
- M. Gholinejad, M. Bahrami, C. Nájera, A fluorescence active catalyst support comprising carbon quantum dots and magnesium oxide doping for stabilization of palladium nanoparticles: application as a recoverable catalyst for Suzuki reaction in water, *Mol. Catal.* 433 (2017) 12–19.
- M. Korzec, P. Bartczak, A. Niemczyk, J. Szade, M. Kapkowski, P. Zenderowska, K. Balin, J. Lelątko, J. Polanski, Bimetallic nano-Pd/PdO/Cu system as a highly effective catalyst for the Sonogashira reaction, *J. Catal.* 313 (2014) 1–8, <https://doi.org/10.1016/j.jcat.2014.02.008>.
- S. Chouzier, M. Gruber, L. Djakovitch, New hetero-bimetallic Pd-Cu catalysts for the one-pot indole synthesis via the Sonogashira reaction, *J. Mol. Catal. A Chem.* 212 (2004) 43–52, <https://doi.org/10.1016/j.molcata.2003.11.027>.
- A. Corma, H. García, A. Primo, Palladium and copper supported on mixed oxides derived from hydrocalcite as reusable solid catalysts for the Sonogashira coupling, *J. Catal.* 241 (2006) 123–131, <https://doi.org/10.1016/j.jcat.2006.04.021>.
- L.M. Tan, Z.Y. Sem, W.Y. Chong, X. Liu, W.L. Kwan, C.L.K. Lee, Hendra, Continuous flow Sonogashira C-C coupling using a heterogeneous palladium-copper dual reactor, *Org. Lett.* 15 (2013) 65–67, <https://doi.org/10.1021/ol303046e>.
- C. Rossy, E. Fouquet, F.X. Felpin, Practical synthesis of indoles and benzofurans in water using a heterogeneous bimetallic catalyst, *Beilstein J. Org. Chem.* 9 (2013) 1426–1431, <https://doi.org/10.3762/bjoc.9.160>.
- C. Rossy, J. Majimel, M.T. Delapierre, E. Fouquet, F.X. Felpin, Palladium and copper-supported on charcoal: a heterogeneous multi-task catalyst for sequential Sonogashira-click and click-heck reactions, *J. Organomet. Chem.* 755 (2014) 78–85, <https://doi.org/10.1016/j.jorganchem.2014.01.006>.
- D. Sengupta, J. Saha, G. De, B. Basu, Pd/Cu bimetallic nanoparticles embedded in macroporous ion-exchange resins: an excellent heterogeneous catalyst for the Sonogashira reaction, *J. Mater. Chem. A* 2 (2014) 3986–3992, <https://doi.org/10.1039/c3ta14916a>.
- M. Gholinejad, N. Jeddi, B. Pullithadathil, Agarose functionalized phosphorus ligand for stabilization of small-sized palladium and copper nanoparticles: efficient heterogeneous catalyst for Sonogashira reaction, *Tetrahedron* 72 (2016) 2491–2500, <https://doi.org/10.1016/j.tet.2016.03.085>.
- C. Evangelisti, A. Balerna, R. Psaro, G. Fusini, A. Carpi, M. Benfatto, Characterization of a poly-4-vinylpyridine-supported CuPd bimetallic catalyst for Sonogashira coupling reactions, *ChemPhysChem* 18 (2017) 1921–1928, <https://doi.org/10.1002/cphc.201700215>.
- Q. Liu, M. Xu, J. Zhao, Z. Yang, C. Qi, M. Zeng, R. Xia, X. Cao, B. Wang, Microstructure and catalytic performances of chitosan intercalated montmorillonite supported palladium (0) and copper (II) catalysts for Sonogashira reactions, *Int. J. Biol. Macromol.* 113 (2018) 1308–1315, <https://doi.org/10.1016/j.jbiomac.2018.03.066>.
- A.V. Rassolov, G.N. Baeva, I.S. Mashkovsky, A.Y. Stakheev, PdCu/Al₂O₃ catalyst for Sonogashira cross-coupling: effect of a Pd/Cu ratio on the catalytic performance, *Mendelev Commun.* 28 (2018) 538–540, <https://doi.org/10.1016/j.mencom.2018.09.030>.
- M. Gholinejad, F. Khosravi, M. Afrasi, J.M. Sansano, C. Nájera, Applications of bimetallic PdCu catalysts, *Catal. Sci. Technol.* 11 (2021) 2652–2702, <https://doi.org/10.1039/c0cy00000a>.

- doi.org/10.1039/d0cy02339f.
- [40] Y.S. Feng, J.J. Ma, Y.M. Kang, H.J. Xu, PdCu nanoparticles supported on graphene: an efficient and recyclable catalyst for reduction of nitroarenes, *Tetrahedron* 70 (2014) 6100–6105, <https://doi.org/10.1016/j.tet.2014.04.034>.
- [41] H. Göksu, N. Zengin, H. Burhan, K. Cellat, F. Şen, A novel hydrogenation of nitroarene compounds with multi wall carbon nanotube supported palladium/copper nanoparticles (PdCu@MWCNT NPs) in aqueous medium, *Sci. Rep.* 10 (2020) 1–8, <https://doi.org/10.1038/s41598-020-64988-0>.
- [42] X. Tan, J. Qin, Y. Li, Y. Zeng, G. Zheng, F. Feng, H. Li, Self-supporting hierarchical PdCu aerogels for enhanced catalytic reduction of 4-nitrophenol, *J. Hazard. Mater.* 397 (2020) 1–8, <https://doi.org/10.1016/j.jhazmat.2020.122786>.
- [43] B. Coq, F. Figueras, Bimetallic palladium catalysts: influence of the co-metal on the catalyst performance, *J. Mol. Catal. A Chem.* 173 (2001) 117–134, [https://doi.org/10.1016/S1381-1169\(01\)00148-0](https://doi.org/10.1016/S1381-1169(01)00148-0).
- [44] J.H. Sinfelt, Catalysis by alloys and bimetallic clusters, *Acc. Chem. Res.* 10 (1977) 15–20, <https://doi.org/10.1021/ar50109a003>.
- [45] R.K. Rai, D. Tyagi, K. Gupta, S.K. Singh, Activated nanostructured bimetallic catalysts for C-C coupling reactions: recent progress, *Catal. Sci. Technol.* 6 (2016) 3341–3361, <https://doi.org/10.1039/c5cy02225h>.
- [46] A. Phan, C.J. Doonan, F.J. Uribe-Romo, C.B. Knobler, O. Keeffe, M. Yaghi, O.M. Acc. Chem. Res. 43 (2010) 58–67.
- [47] S. Yang, B. Pattengale, E.L. Kovrigin, J. Huang, Photoactive zeolitic imidazolate framework as intrinsic heterogeneous catalysts for light-driven hydrogen generation, *ACS Energy Lett.* 2 (2017) 75–80, <https://doi.org/10.1021/acsenergylett.6b00540>.
- [48] H. Hayashi, A.P. Côté, H. Furukawa, M. O’Keeffe, O.M. Yaghi, Zeolite A imidazolate frameworks, *Nat. Mater.* 6 (2007) 501–506, <https://doi.org/10.1038/nmat1927>.
- [49] F. Zhang, Y. Wei, X. Wu, H. Jiang, W. Wang, H. Li, Hollow zeolitic imidazolate framework nanospheres as highly efficient cooperative catalysts for [3 + 3] cycloaddition reactions, *J. Am. Chem. Soc.* 136 (2014) 13963–13966, <https://doi.org/10.1021/ja506372z>.
- [50] H. Sun, B. Tang, P. Wu, Two-dimensional zeolitic imidazolate framework/carbon nanotube hybrid networks modified proton exchange membranes for improving transport properties, *ACS Appl. Mater. Interfaces* 9 (2017) 35075–35085, <https://doi.org/10.1021/acsmi.7b13013>.
- [51] M. Gholinejad, Z. Naghsbandi, J.M. Sansano, Co/Cu bimetallic ZIF as New heterogeneous catalyst for reduction of nitroarenes and dyes, *Appl. Organomet. Chem.* 34 (2020) 1–10, <https://doi.org/10.1002/aoc.5522>.
- [52] B. Chen, Z. Yang, Y. Zhu, Y. Xia, Zeolitic imidazolate framework materials: recent progress in synthesis and applications, *J. Mater. Chem. A* 2 (2014) 16811–16831, <https://doi.org/10.1039/c4ta02984d>.
- [53] M.U.A. Prathap, S. Gunasekaran, Rapid and scalable synthesis of zeolitic imidazole framework (ZIF-8) and its use for the detection of trace levels of nitroaromatic explosives, *Adv. Sustain. Syst.* 2 (2018) 1800053.
- [54] A. Zhou, R.M. Guo, J. Zhou, Y. Dou, Y. Chen, J.R. Li, Pd@ZIF-67 derived recyclable Pd-based catalysts with hierarchical pores for high-performance heck reaction, *ACS Sustain. Chem. Eng.* 6 (2018) 2103–2111, <https://doi.org/10.1021/acssuschemeng.7b03525>.
- [55] Y. Wang, Y. Zeng, X. Wu, M. Mu, L. Chen, A novel Pd-Ni bimetallic synergistic catalyst on ZIF-8 for Sonogashira coupling reaction, *Mater. Lett.* 220 (2018) 321–324, <https://doi.org/10.1016/j.matlet.2018.03.006>.
- [56] H. Mao, W. Zhang, W. Zhou, B. Zou, B. Zheng, S. Zhao, F. Huo, Hybridization of metal nanoparticles with metal-organic frameworks using protein as amphiphilic stabilizer, *ACS Appl. Mater. Interfaces* 9 (2017) 24649–24654, <https://doi.org/10.1021/acsmi.7b06754>.
- [57] R.R. Salunkhe, J. Tang, Y. Kamachi, T. Nakato, J.H. Kim, Y. Yamauchi, Asymmetric supercapacitors using 3D nanoporous carbon and cobalt oxide electrodes synthesized from a single metal-organic framework, *ACS Nano* 9 (2015) 6288–6296, <https://doi.org/10.1021/acsnano.5b01790>.
- [58] J. Song, C. Zhu, B.Z. Xu, S. Fu, M.H. Engelhard, R. Ye, D. Du, S.P. Beckman, Y. Lin, Bimetallic cobalt-based phosphide zeolitic imidazolate framework: CoPx phase-dependent electrical conductivity and hydrogen atom adsorption energy for efficient overall water splitting, *Adv. Energy Mater.* 7 (2017) 1–9, <https://doi.org/10.1002/aenm.201601555>.
- [59] C. Chen, A. Wu, H. Yan, Y. Xiao, C. Tian, H. Fu, Trapping [Pm12O40]3- clusters into pre-synthesized ZIF-67 toward Mo: xOxC particles confined in uniform carbon polyhedrons for efficient overall water splitting, *Chem. Sci.* 9 (2018) 4746–4755, <https://doi.org/10.1039/c8sc01454j>.
- [60] J. He, D. Chen, N. Li, Q. Xu, H. Li, J. He, J. Lu, Controlled fabrication of mesoporous ZSM-5 zeolite-supported PdCu alloy nanoparticles for complete oxidation of toluene, *Appl. Catal. B Environ.* 265 (2020) 118560.
- [61] I.A. Khan, L. Khan, S.I. Khan, A. Badshah, Shape-control synthesis of PdCu nanoparticles with excellent catalytic activities for direct alcohol fuel cells application, *Electrochim. Acta* 349 (2020) 136381, <https://doi.org/10.1016/j.electacta.2020.136381>.
- [62] X. Guo, T. Xing, Y. Lou, J. Chen, Controlling ZIF-67 crystals formation through various cobalt sources in aqueous solution, *J. Solid State Chem.* 235 (2016) 107–112, <https://doi.org/10.1016/j.jssc.2015.12.021>.
- [63] S. Sundriyal, V. Shrivastav, H. Kaur, S. Mishra, A. Deep, High-performance symmetrical supercapacitor with a combination of a ZIF-67/rGO composite electrode and a redox additive electrolyte, *ACS Omega* 3 (2018) 17348–17358, <https://doi.org/10.1021/acsomega.8b02065>.
- [64] T.T. Han, Y.Y. Liu, G.C. Yang, J.F. Ma, One-step encapsulation of functionalized EAQ and TBAQ molecules inside zeolite imidazolate framework-67 and their electrochemical characterizations, *Microporous Mesoporous Mater.* 247 (2017) 177–183, <https://doi.org/10.1016/j.micromeso.2017.04.005>.
- [65] Z.Q. Zhang, J. Huang, L. Zhang, M. Sun, Y.C. Wang, Y. Lin, J. Zeng, Facile synthesis of Cu-Pd bimetallic multipods for application in cyclohexane oxidation, *Nanotechnology* (2014) 25, <https://doi.org/10.1088/0957-4484/25/43/435602>.
- [66] L. Wang, J.J. Zhai, K. Jiang, J.Q. Wang, W. Bi. Cai, Pd-Cu/C electrocatalysts synthesized by one-pot polyol reduction toward formic acid oxidation: structural characterization and electrocatalytic performance, *Int. J. Hydrog. Energy.* 40 (2015) 1726–1734, <https://doi.org/10.1016/j.ijhydene.2014.11.128>.
- [67] A. Khan, M. Ali, A. Ilyas, P. Naik, I.F.J. Vankelecom, M.A. Gilani, M.R. Bilal, Z. Sajjad, A.L. Khan, ZIF-67 filled PDMS mixed matrix membranes for recovery of ethanol via pervaporation, *Sep. Purif. Technol.* 206 (2018) 50–58, <https://doi.org/10.1016/j.seppur.2018.05.055>.
- [68] M. Massoudinejad, M. Ghaderpoori, A. Shahsavani, A. Jafari, B. Kamarehie, A. Ghaderpoury, M.M. Amini, Ethylenediamine-functionalized cubic ZIF-8 for arsenic adsorption from aqueous solution: modeling, isotherms, kinetics and thermodynamics, *J. Mol. Liq.* 255 (2018) 263–268, <https://doi.org/10.1016/j.molliq.2018.01.163>.
- [69] N. Mostafazadeh, A.A. Ghoreyshi, K. Pirzadeh, Optimization of solvothermally synthesized ZIF-67 metal organic framework and its application for Cr (VI) adsorption from aqueous solution, *Iran. J. Chem. Eng.* 15 (2018) 27–47.
- [70] A. Elfiad, F. Galli, L.M. Boukhobza, A. Djadoun, D.C. Boffito, Low-cost synthesis of Cu/α-Fe₂O₃ from natural HFeO₂: application in 4-nitrophenol reduction, *J. Environ. Chem. Eng.* 8 (2020), <https://doi.org/10.1016/j.jece.2020.104214>.
- [71] Z. Naghsbandi, N. Arsalani, M.S. Zakerhamidi, K.E. Geckeler, A novel synthesis of magnetic and photoluminescent graphene quantum dots/MFe₂O₄ (M = Ni, Co) nanocomposites for catalytic application, *Appl. Surf. Sci.* 443 (2018) 484–491, <https://doi.org/10.1016/j.apsusc.2018.02.283>.
- [72] F. Al-Wadaani, A. Omer, M. Abboudi, H.O. Hassani, S. Rakass, M. Messali, M. Benaissa, High catalytic efficiency of nanostructured β-CoMoO₄ in the reduction of the ortho-, meta- and para-nitrophenol isomers, *Molecules* 23 (2018), <https://doi.org/10.3390/molecules23020364>.
- [73] Y. Wang, H. Li, J. Zhang, X. Yan, Z. Chen, Fe₃O₄ and Au nanoparticles dispersed on the graphene support as a highly active catalyst toward the reduction of 4-nitrophenol, *Phys. Chem. Chem. Phys.* 18 (2016) 615–623, <https://doi.org/10.1039/c5cp05336f>.
- [74] J. Zhu, X. Zhang, Z. Qin, L. Zhang, Y. Ye, M. Cao, L. Gao, T. Jiao, Preparation of PdNPs doped chitosan-based composite hydrogels as highly efficient catalysts for reduction of 4-nitrophenol, *Colloids Surf. A Physicochem. Eng. Asp.* 611 (2021) 125889, <https://doi.org/10.1016/j.colsurfa.2020.125889>.
- [75] Y. Cui, X. Guo, X. Lai, H. Sun, B. Liang, W. Hou, X. Liu, L. Wang, Green synthesis of jujube-polysaccharide-stabilized gold nanoparticles for reduction of 4-nitrophenol, *ChemistrySelect* 4 (2019) 11483–11487, <https://doi.org/10.1002/slct.201902531>.
- [76] A.T.E. Vilián, S.R. Choe, K. Giribabu, S.C. Jang, C. Roh, Y.S. Huh, Y.K. Han, Pd nanospheres decorated reduced graphene oxide with multi-functions: highly efficient catalytic reduction and ultrasensitive sensing of hazardous 4-nitrophenol pollutant, *J. Hazard. Mater.* 333 (2017) 54–62, <https://doi.org/10.1016/j.jhazmat.2017.03.015>.
- [77] L. Zhi, H. Liu, Y. Xu, D. Hu, X. Yao, J. Liu, Pyrolysis of metal-organic framework (CuBTC) decorated filter paper as a low-cost and highly active catalyst for the reduction of 4-nitrophenol, *Dalton Trans.* 47 (2018) 15458–15464, <https://doi.org/10.1039/C8DT03327G>.
- [78] X. Sun, P. He, Z. Gao, Y. Liao, S. Weng, Z. Zhao, H. Song, Z. Zhao, Multi-crystalline N-doped Cu/Cu₂O/C foam catalyst derived from alkaline N-coordinated HKUST-1/CMC for enhanced 4-nitrophenol reduction, *J. Colloid Interface Sci.* 553 (2019) 1–13, <https://doi.org/10.1016/j.jcis.2019.06.004>.
- [79] C. Chu, S. Rao, Z. Ma, H. Han, Copper and cobalt nanoparticles doped nitrogen-containing carbon frameworks derived from CuO-encapsulated ZIF-67 as high-efficiency catalyst for hydrogenation of 4-nitrophenol, *Appl. Catal. B Environ.* 256 (2019) 117792, <https://doi.org/10.1016/j.apcatb.2019.117792>.
- [80] X. Zhang, N. Wang, L. Geng, J. Fu, H. Hu, D. Zhang, B. Zhu, J. Carozza, H. Han, Facile synthesis of ultrafine cobalt oxides embedded into N-doped carbon with superior activity in hydrogenation of 4-nitrophenol, *J. Colloid Interface Sci.* 512 (2018) 844–852, <https://doi.org/10.1016/j.jcis.2017.11.005>.
- [81] C.S. Budi, J.R. Deka, W.C. Hsu, D. Saikia, K.T. Chen, H.M. Kao, Y.C. Yang, Bimetallic Co/Zn zeolitic Imidazolate Framework ZIF-67 Supported Cu nanoparticles: An excellent Catalyst For Reduction of Synthetic Dyes and Nitroarenes, *Elsevier*, 2021, <https://doi.org/10.1016/j.jhazmat.2020.124392>.
- [82] H. Zhao, L. Zhao, Magnetic N-doped Co-carbon composites derived from metal organic frameworks as highly efficient catalysts for p-nitrophenol reduction reaction, *Dalton Trans.* 47 (2018) 3321–3328, <https://doi.org/10.1039/c7dt04272h>.